

Pygmy Dipol Resonances as a Manifestation of the Structure of the Neutron-Rich Nuclei

N. Tsoneva^a ^{*}, H. Lenske^a and Ch. Stoyanov^b

^aInstitut für Theoretische Physik, Universität Gießen, Heinrich-Buff-Ring 16, D-35392 Gießen, Germany

^bInstitute for Nuclear Research and Nuclear Energy, 1784 Sofia, Bulgaria

Dipole excitations in neutron-rich nuclei below the neutron threshold are investigated. The method is based on Hartree-Fock-Bogoliubov (HFB) and Quasiparticle-Phonon Model (QPM) theory. Of our special interest are the properties of the low-lying 1^- *Pygmy Resonance* and the two-phonon quadrupole-octupole 1^- states in Sn-isotopes including exploratory investigations for the experimentally unknown mass regions. In particular we investigate the evolution of the dipole strength function with the neutron excess. The use of HFB mean-field potentials and s.p. energies is found to provide a reliable extrapolation into the region off stability.

1. Introduction

The understanding of the structure of atomic nuclei at extreme isospin is a challenge for nuclear physics which has become achievable on a large scale after the modern experimental nuclear structure facilities [1] came into operation. For the theoretical studies of such systems of importance is the search for suitable observables. One promising choice for the investigation for example of neutron-rich nuclei is to look after their excitation modes and trying to find correlations e.g. of transition probabilities and excitation energies with the size and shape of the neutron skin. The appearance of low-energy electric dipole strength is a genuine feature of neutron-rich nuclei, seen recently in high-precision photon scattering experiments already in stable nuclei with small [2,3] and moderate [4] neutron excess. These so-called *Pygmy Dipole Resonances (PDR)* are located close to the neutron threshold, forming in presently accessible medium- and heavy-mass nuclei a clustering of states in the region of $E_x \sim 5.5 \div 8$ MeV. Although carrying only a small fraction of the full dipole strength these states are of particular interest because they are reflecting the motion of the neutron skin against the core of normal nuclear matter. As discussed in [4], their nature is completely different from the representation where proton and neutron fluids as a whole move against each other, giving rise to the prominent isovector Giant Dipole Resonance (GDR).

The PDR mode has to be distinguished from the other known low-energy isoscalar dipole excitation, namely the two-phonon 1^- states resulting from the anharmonic inter-

^{*}Also at Institute for Nuclear Research and Nuclear Energy, 1784 Sofia, Bulgaria

actions of the lowest 2^+ and 3^- states in a nucleus. A comprehensive collection of data on the latter and overview of the widely used experimental methods is given in [5]. The anharmonicities are reflecting the intrinsic fermionic structure of the nuclear phonons thus deviating from ideal bosons. A model taking into account that nuclear phonons are formed by exciting at least two quasiparticles (corresponding to a one particle one hole state (1p1h)) which interact by a residual two-body NN-interaction is the QPM [6,7] worked out and applied systematically [8,9,10], e.g. also in the recent PDR investigations in the stable $^{116,124}\text{Sn}$ [11] and ^{208}Pb [4] nuclei. Other applications of the QPM to low-energy dipole strength [12,13,14] have led to very good description of data thus giving confidence on the reliability of the model for such investigations.

Most likely, the QPM approach is at present the only available method for a unified description of low-energy single and multiple phonon states. The use of schematic interactions of separable form and with empirical coupling constants is a detail which in principle could be improved on. Recently, finite rank approximation for Skyrme interaction was incorporated in the formalism of QPM [15]. Work in this direction is in progress but since the investigations in this paper are mainly directed to an exploratory study of the evolution of the PDR modes with neutron excess we use the standard form of the QPM.

Here, the mean-field part, however, is treated microscopically by incorporating HFB results on single particle energies and potentials as input for the QPM calculations.

The interest on the region around the $N=82$ shell closure has arisen recently [16,17,18] and will further increase with the new experimental opportunities on REX-ISOLDE, MAFF and also the coming-up GSI project. In this manuscript we have presented calculations for the neutron-rich Sn isotopes with neutron number $N=70 \div 82$ as an exploratory investigation in experimentally less or even unknown regions.

2. Description of the method

For the extrapolation of the QRPA and QPM calculations into unknown mass regions a reliable description of the ground state properties is necessary. Because of the numerical constraints set by the QPM a semi-microscopic approach is chosen. The model Hamiltonian is written as:

$$H = H_{MF} + H_M^{ph} + H_{SM}^{ph} + H_M^{pp} , \quad (1)$$

where $H_{MF} = H_{sp} + H_{pair}$ represents the mean-field part describing the motion of independent quasiparticles in a static potential and interacting in the particle-particle (p-p) channel through the monopole pairing interaction H_{pair} . H_{MF} is to be identified with the HFB Hamiltonian discussed in [19,20]. For practical purposes, however, we use here a re-parameterization of the HFB mean-field in terms of Wood-Saxon potential- U_{WS} fitted to the HFB mean-field such that the single-particle energies are reproduced. Also, the pairing part is simplified by using the conventional constant matrix element approach which close to the Fermi level is a reliable approximation.

H_M^{ph} and H_{SM}^{ph} are residual interactions taken as a sum of isoscalar and isovector separable multipole and spin-multipole interactions in the particle-hole channel. H_M^{pp} is the sum of the multipole pairing interactions in the particle-particle (p-p) channel.

In practice, for a given nucleus of mass A the depth of the central and spin-orbit potentials, radius and diffusivity parameters of U_{WS} are adjusted separately for protons

and neutrons to the corresponding single particle separation energies, the total binding energy [21], the charge radii and (relative) differences of proton and neutron root-mean-square (RMS) radii,

$$\delta r = \sqrt{\langle r^2 \rangle_n} - \sqrt{\langle r^2 \rangle_p} \quad (2)$$

indicating the thickness of the neutron skin. The results from this procedure are compared to experimental values from the compilation of Audi and Wapstra [21] and the recent investigations of neutron skins by Krasznahorkay et al. by charge exchange reactions [22], respectively. For both observables the agreement of theory and data is very satisfactory as it is seen from Fig.1.

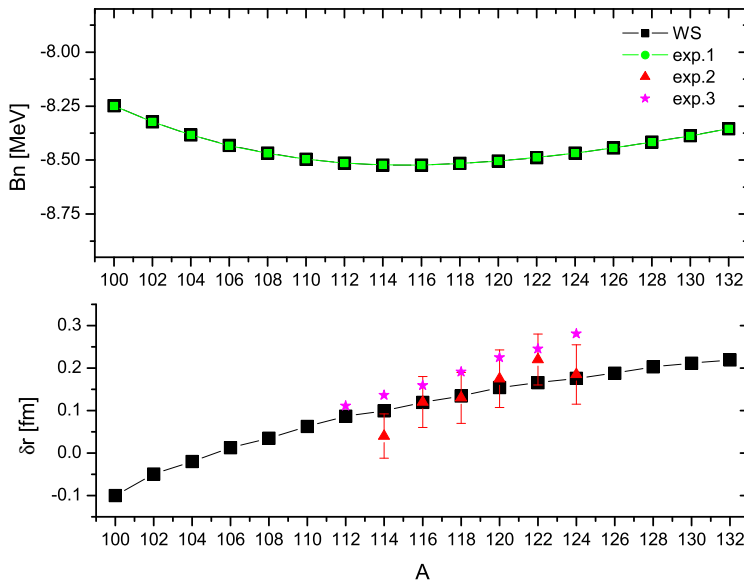


Figure 1. Ground state properties of the Sn isotopes. In the upper panel the total nuclear binding energies per particle are compared to the values from the Audi-Wapstra compilation [21]. In the lower panel the differences of proton and neutron rms radii are compared to the experimental values obtained from charge exchange reactions in ref. [22].

The model Hamiltonian is diagonalized assuming a spherical 0^+ ground state which leads to an orthonormal set of wave functions with good total angular momentum JM. For even-even nuclei these wave functions are a mixture of one-, two- and three-phonon components in the following way [13]:

$$\Psi_\nu(JM) = \left\{ \sum_i R_i(J\nu) Q_{JM i}^+ + \sum_{\substack{\lambda_1 i_1 \\ \lambda_2 i_2}} P_{\lambda_2 i_2}^{\lambda_1 i_1}(J\nu) [Q_{\lambda_1 \mu_1 i_1}^+ \times Q_{\lambda_2 \mu_2 i_2}^+]_{JM} \right\} \quad (3)$$

$$+ \sum_{\substack{\lambda_1 i_1 \lambda_2 i_2 \\ \lambda_3 i_3 I}} T_{\lambda_3 i_3}^{\lambda_1 i_1 \lambda_2 i_2 I}(J\nu) \left[\left[Q_{\lambda_1 \mu_1 i_1}^+ \otimes Q_{\lambda_2 \mu_2 i_2}^+ \right]_{IK} \otimes Q_{\lambda_3 \mu_3 i_3}^+ \right]_{JM} \left. \right\} \Psi_0$$

where R, P and T are unknown amplitudes, and ν labels the number of the excited states.

The model basis includes the natural parity 1^- , 2^+ , 3^- , 4^+ , 5^- phonons only. For the description of the structure of each of the excited states we use a wave function from Eq. (3). For the case of 1^- states one-phonon configurations up to $E_x=20$ MeV are included. This allows us to take into account microscopically the influence of core polarization on the low-lying 1^- states without any phenomenologically induced effective charges. The two- and three-phonon configurations are truncated up to 4.5 MeV for the calculation of the quadrupole-octupole 1^- state for the proper comparison with the available NRF data [12]. For the QPM calculations between $4.5 \div 8$ MeV the two- and three-phonon basis is limited to states up to $E_x=8.5$ MeV and 8 MeV, respectively.

3. Results

The new method we have applied for the determination of the ground state properties allows to investigate the evolution of the dipole strength function with the neutron excess.

Of our particular interest are the one-phonon 1^- states below the neutron threshold with excitation energies up to 8 MeV in $^{120 \div 126}\text{Sn}$ and up to 7.5 MeV in $^{128 \div 132}\text{Sn}$ respectively. In fact, the first three 1^- QRPA states enter in this energy region. They are rather well separated from the other higher-lying one-phonon 1^- states by an energy gap of more than 1.3 MeV. The first QRPA state contains mainly a neutron two-quasiparticle ($\approx 99.7\%$) component while the mixing between different two-quasiparticle neutron and proton configurations (the contribution of the protons is about 0.2% only) becomes more important for the second and the third QRPA states. These states we identify with the PDR which in the case of our QRPA calculations is located in the energy region $5.9 \div 7$ MeV. The obtained neutron structure of the 1^- QRPA states is in agreement with the explanation of the PDR in other nuclei obtained before by DFT [23], RQRPA [18] and QPM[4] theory.

This remarkable stability of the wave functions is similar to what is found in theoretical studies of the GDR. In medium and heavy nuclei the model independent Thomas-Reiche-Kuhn limit of the dipole EWSR is found to be almost exhausted already by RPA or QRPA calculations, indicating the dominance of $1p1h$ or two-quasiparticle structures and agreeing with experiment. However, we emphasize that the PDR states are of predominantly isoscalar (or eventually mixed isospin) character as already pointed out in [4]. Hence, the PDR states cannot be considered as belonging simply to the low-energy tail of the *isovector* GDR. Rather, this dipole modes are of a genuine character which cannot be deduced by extrapolations from the GDR region.

As a general result we find a correlation of the total PDR strength and the number of the neutrons (presented on Fig.2a). The value of the total PDR strength increases in going to the heavier tin isotopes, up to ^{132}Sn . At the same time the centroid energies show an opposite behavior (Fig.2b).

We have extended the QRPA calculations in terms of QPM, which allows us to investigate the properties of the lowest-lying two-phonon quadrupole-octupole 1^- states

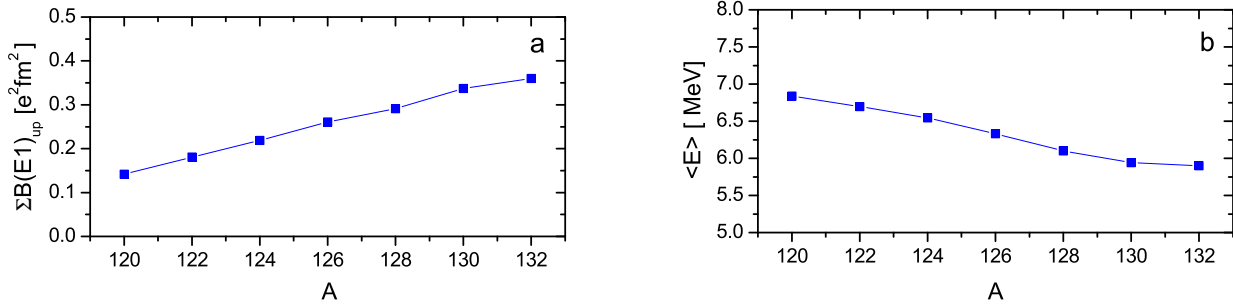


Figure 2. QRPA calculations on the PDR a)total strength and b)centroid energy as a function of the neutron access in $^{120-132}\text{Sn}$ isotopes.

in $^{120-130}\text{Sn}$ isotopes as well.

A proper description of the quadrupole $J^\pi=2_1^+$ and octupole $J^\pi=3_1^-$ states is important with respect to the two-phonon $J^\pi=1^-$ state. The calculated energies and transition probabilities of the first 2^+ , 3^- states are presented in Table 1, where also the known experimental data are shown [24]. A good agreement between the calculations and the experiment is obtained.

The properties of the lowest lying 1^- states have been investigated in the frame of QPM. The energy varies from $E_x=3.203$ MeV to $E_x=4.115$ MeV in $^{120-130}\text{Sn}$ (see Table 1). In these isotopes the structure of the 1^-_1 states is predominantly by about 88-93% of two-phonon quadrupole-octupole character. Since with increasing neutron number the energy of the latter becomes larger, certain other, higher-lying, two-phonon configurations start to contribute as well. The three-phonon configurations are most important for the investigated lower mass number Sn isotopes. This effect is connected with the decrease of the collectivity of the nuclear excitations when we come to the closed $N=82$ shell. The $E1$ transitions from the two-phonon 1^- state to the ground state and between 3^-_1 and 2_1^+ excited states are an example of 'boson forbidden' transitions with one- or two-phonon exchange [14]. The QPM calculations on the $B(E1; 0^+ \rightarrow 1^-_1)$ and $B(E1; 3^-_1 \rightarrow 2_1^+)$ transition probabilities are in a good agreement with the available experimental data.

A comparison between the QRPA and QPM dipole strength distribution below the neutron threshold in ^{122}Sn and ^{130}Sn is presented in Fig.3. The lowest QPM 1^- state has no QRPA counterpart because, as discussed above, it is of quadrupole-octupole two-phonon structure. While in QRPA the dipole strength in the investigated Sn isotopes is concentrated in three dipole states the QPM phonon interactions lead to fragmentation - in this case about 80 states - and dissipation seen as a reduction of the total one-phonon content of the multi-phonon eigenstates.

These quenching and fragmentation effects are directly observable in the $B(E1)$ transition probabilities to the ground state which are determined by the one-phonon components

Table 1

QPM results for the energies and the reduced $B(E1)$, $B(E2)$ and $B(E3)$ transition probabilities of the first 1^- , 2^+ and 3^- states in $^{120\div 130}\text{Sn}$ isotopes. A comparison with the experimental data is presented [11].

Nucl.	Energy [MeV]	Trans.		$B(E1; I_\nu^\pi \rightarrow J_{\nu'}^{\pi'}) [10^{-3} \text{ e}^2\text{fm}^2]$			
		$J_{\nu'}^{\pi'}$	Exp.	QPM	$E\lambda$	I_ν^π	$B(E2; I_\nu^\pi \rightarrow J_{\nu'}^{\pi'}) [10^4 \text{ e}^2\text{fm}^4]$
		$J_{\nu'}^{\pi'}$	Exp.	QPM	I_ν^π	Exp.	$B(E3; I_\nu^\pi \rightarrow J_{\nu'}^{\pi'}) [10^6 \text{ e}^2\text{fm}^6]$
^{120}Sn	2_1^+	1.171	1.171	E2	0_1^+	0.200(3)	0.193
				E1	3_1^-	2.02(17)	1.82
	3_1^-	2.401	2.424	E3	0_1^+	0.115(15)	0.110
	1_1^-	3.279	3.203	E1	0_1^+	7.6(51)	7.6
^{122}Sn	2_1^+	1.141	1.137	E2	0_1^+	0.194(11)	0.190
				E1	3_1^-	2.24(14)	2.06
	3_1^-	2.493	2.486	E3	0_1^+	0.092(10)	0.099
	1_1^-	3.359	3.281	E1	0_1^+	7.16(54)	7.02
^{124}Sn	2_1^+	1.132	1.133	E2	0_1^+	0.166(4)	0.174
				E1	3_1^-	2.02(16)	1.98
	3_1^-	2.614	2.645	E3	0_1^+	0.073(10)	0.087
	1_1^-	3.490	3.549	E1	0_1^+	6.08(66)	6.27
^{126}Sn	2_1^+	1.141	1.151	E2	0_1^+	-	0.140
				E1	3_1^-	-	1.74
	3_1^-	2.720	2.792	E3	0_1^+	-	0.079
	1_1^-	-	3.856	E1	0_1^+	-	5.8
^{128}Sn	2_1^+	1.168	2.217	E2	0_1^+	-	0.097
				E1	3_1^-	-	1.07
	3_1^-	-	2.849	E3	0_1^+	-	0.081
	1_1^-	-	4.115	E1	0_1^+	-	5.56
^{130}Sn	2_1^+	1.221	1.204	E2	0_1^+	-	0.066
				E1	3_1^-	-	1.11
	3_1^-	-	2.861	E3	0_1^+	-	0.098
	1_1^-	-	4.094	E1	0_1^+	-	5.53

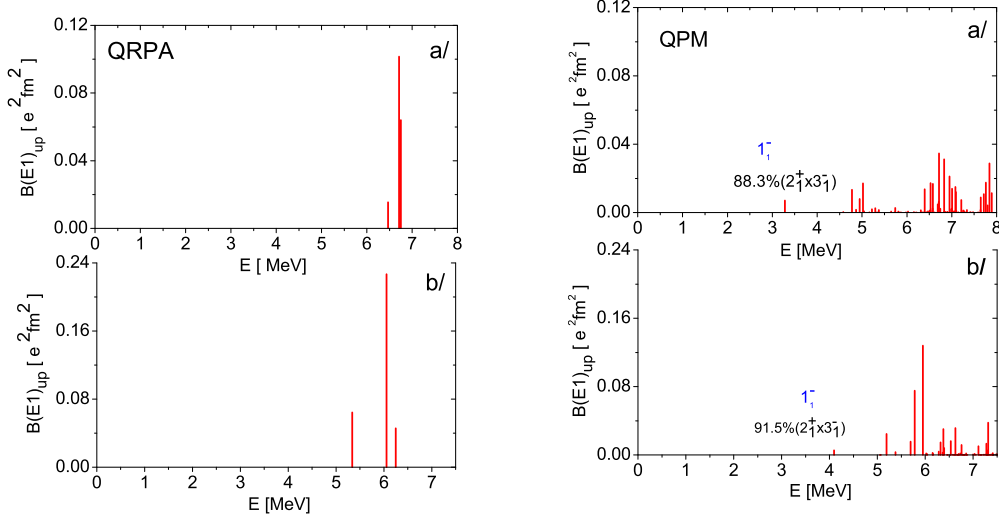


Figure 3. QRPA and QPM calculations of the E1 strength distribution in a/ ^{122}Sn and b/ ^{130}Sn below the neutron threshold.

of the excited states: reductions in the one-phonon state amplitudes are reflected in a corresponding suppression of the ground state transition matrix elements. In ^{122}Sn and ^{130}Sn about 85% of the PDR one-phonon strength is exhausted in the energy intervals up to 8 MeV and 7.5 MeV, respectively. Compared to the calculations in [11] we find less fragmentation because the size of our two- and three-phonon configuration spaces are somewhat smaller. However, the total E1 strength in the investigated energy interval is in very reasonable agreement with the available experimental data in ^{124}Sn .

4. Summary and Conclusions

A new method based on HFB and QPM theory was applied for the study of the neutron-rich tin isotopes. From our calculations on $^{120}\text{Sn} \div 132\text{Sn}$ we obtained low-energy dipole strength in the energy region 5.9 \div 6.9 MeV concentrated in a narrow energy interval such that a *pygmy dipole resonance* (PDR) can be identified. The correlation of the PDR excitation energy and transition strength with the neutron excess was investigated. Its strength increases with the neutron number while the centroid energy decreases. By comparison to the radii of HFB ground state densities a correlation with the size of the neutron skin could be identified. An important step in understanding the dipole spectra is to disentangle the PDR states from the low-energy two-phonon dipole states. In our calculations this was achieved by using the QPM approach with up to three-phonon configurations.

For the experimentally unknown nuclei the excitation energy of the two-phonon 1-

state and B(E1) transition probability are predicted. The method will be applied for other regions of nuclei.

The authors of the paper wish to acknowledge the discussions they had with U. Kneissl and H.H. Pitz. This work is supported by DFG, contract Le439/5.

REFERENCES

1. P.G. Hansen et al., Ann. Rev. Phys. Sci. (N.Y.) **45** (1995) 591.
2. T. Hartmann et al., Phys. Rev. **C65** (2002) 034301.
3. A. Zilges et al., Phys. Lett. **B 542** (2002) 43.
4. N. Ryezayeva et al., Phys. Rev. Lett. **89** (2002) 272502.
5. H.H. Pitz, *ISNSP 2001, University of Göttingen, Germany*, ed. R. Casten et al., p.61.
6. V.G. Soloviev, *Theory of complex nuclei* (Oxford: Pergamon Press, 1976).
7. V.G. Soloviev, *Theory of Atomic Nuclei: Quasiparticles and Phonons*, (Inst. of Phys. Publ., Bristol, 1992).
8. A. I. Vdovin et al., Sov. J. Part. Nucl., **14** (1983) 237.
9. V. V. Voronov et al., Sov. J. Part. Nucl., **14** (1983) 1380.
10. S. Gales et al., Phys. Rep. **166** (1988) 125.
11. K. Govaert et al., Phys. Rev. **C57** (1998) 2229.
12. J. Bryssinck et al., Phys. Rev. **C59** (1999) 1930.
13. M. Grinberg et al., Nucl. Phys. **A573** (1994) 231.
14. V.Yu. Ponomarev et al., Nucl. Phys. **A635** (1998) 470.
15. A. P. Severyukhin et al., Phys. Rev. **C66** (2002) 034304.
16. L. Coraggio et al., Phys. Rev. **C65** (2002) 051306.
17. J. Terasaki et al., Phys. Rev. **C66** (2002) 054313.
18. N. Paar et al., Phys. Rev. **C67** (2003) 034312.
19. F. Hofmann et al., Phys. Rev. **C57** (1998) 2281.
20. H. Lenske et al., Rep. Prog. Nucl. Part. Phys. **46** (2001) 187,
e-Print Archive: nucl-th/0012082.
21. G. Audi et al., Nucl. Phys. **A595** (1995) 409.
22. A. Krasznahorkay et al., Phys. Rev. Lett. **82** (1999) 3216; A. Krasznahorkay et al., *INPC 2001*, edited by E. Norman et al., p.751.
23. J. Chambers et al., Phys. Rev. **C50** (1994) R2671.
24. S. Raman et al., At. Data Nucl. Data Tabl. **78** (2001); T. Kibédi et al., At. Data Nucl. Data Tabl. **80** (2002).